



Resolving resource partitioning in parrotfishes (Scarini) using microhistology of feeding substrata

Georgina M. Nicholson¹ · Kendall D. Clements¹

Received: 24 February 2020 / Accepted: 26 May 2020 / Published online: 9 June 2020
© Springer-Verlag GmbH Germany, part of Springer Nature 2020

Abstract Parrotfishes (Scarini) are considered key agents in coral reef health and recovery, but the drivers of parrotfish–coral dynamics remain contentious. The prevailing view of parrotfishes as ecosystem engineers is based on the perceived removal of algal turf, macroalgae and sediment, but these are effects of feeding, not causes. The recent proposal that most parrotfishes are ‘microphages’ that target microscopic photoautotrophs (particularly cyanobacteria) identifies the need to resolve dietary targets at a microscopic scale. Here, we investigate parrotfish dietary targets by posing the following two questions: (1) are microscopic photoautotrophs the most consistent and dominant elements of the prey community, and (2) do the prey community and substratum taphonomy vary between parrotfish species? In order to identify and quantify dietary targets, five parrotfish species were followed until focused feeding was observed at Lizard Island on the Great Barrier Reef, Australia. Feeding sites were photographed in situ and extracted as substratum bite cores. Cores were analysed microscopically to identify and quantify all epilithic photoautotrophs. Endolithic photoautotrophs accessible to excavating parrotfish were also investigated by vacuum-embedding cores with epoxy resin followed by decalcification to expose endolith microborings. The dominant functional groups of epilithic biota on the cores were tufted cyanobacteria, turfing algae and crustose coralline algae

(CCA). The only consistent feature across all cores was the high density of filamentous cyanobacteria, supporting the view that these parrotfishes target microphotoautotrophs. Macroalgae was absent or a minor component on cores, supporting the hypothesis that parrotfishes avoid larger algae. The microchlorophyte *Ostreobium* was the dominant photoautotrophic euendolith (true borer) in the cores of the excavating parrotfish *Chlorurus microrhinos*. Significant differences in CCA coverage, turf height and substrate taphonomy were found among the five parrotfish species, suggesting that interspecific resource partitioning is based on successional stage of feeding substrata.

Keywords Parrotfish · Coral reef · *Ostreobium* · Cyanobacteria · Herbivory · Algae

Introduction

Herbivorous fishes have long been considered integral to the functioning and maintenance of coral reef systems (Odum and Odum 1955; Ogden and Lobel 1978; Steneck 1983, 1995; Choat 1991). Herbivory by parrotfish has been identified as critical to coral reef health (Bonaldo et al. 2014; Bozec et al. 2016), and parrotfish are seen as ecosystem engineers able to modify the physical environment sensu Jones et al. (1994, 2010). Parrotfish are perceived as key factors of prevention and recovery in macroalgal phase shifts (Bellwood et al. 2004, 2006; Mumby et al. 2006; Steneck et al. 2014; Adam et al. 2015a). Parrotfishes are important agents of reef bioerosion, sediment generation and sediment transport (Mallela and Fox 2018), all of which are significant drivers of reef geomorphology (Perry et al. 2015; Morgan and Kench 2016). In light of their perceived importance to coral reef

Electronic supplementary material The online version of this article (<https://doi.org/10.1007/s00338-020-01964-0>) contains supplementary material, which is available to authorized users.

✉ Georgina M. Nicholson
gmic606@aucklanduni.ac.nz

¹ School of Biological Sciences, University of Auckland, Private Bag 92019, Auckland, New Zealand

health, bans on fishing for herbivores, particularly parrotfishes, have been introduced and herbivore management areas (HMA) have been proposed to mitigate macroalgal dominance (Mumby 2006; Chung et al. 2019; Williams et al. 2019). The view that parrotfish are critical to coral reef ecosystems carries assumptions about their feeding behaviour and diet. Nonetheless, parrotfish diets (i.e. nutritional targets) remain poorly characterized (Clements et al. 2017). Resolving this is therefore a research priority and is the subject of the present study.

Most studies on coral reef trophodynamics, ecosystem functioning and responses to disturbance use the feeding categories ‘scraper’, ‘browser’ and ‘excavator’ (Bellwood and Choat 1990; Bonaldo et al. 2014) rather than dietary categories for parrotfishes (Ong and Holland 2010; Stuart-Smith et al. 2013; Melgarejo-Damián et al. 2018). The diet of grazing (scraping and excavating) parrotfish is often described as ‘whole EAM’ (e.g. Steneck et al. 2017; Bellwood et al. 2018), where the ‘Epilithic Algal Matrix’ is defined as short, turf-forming filamentous algae (< 1 cm high), macroalgal spores, microalgae, sediment, detritus and associated fauna (Wilson et al. 2003; Hoey and Bellwood 2010; Bonaldo et al. 2014). Under this view grazing parrotfish, surgeonfish and rabbitfish are seen as dietary generalists, some of which differ in feeding microhabitat (Brandl and Bellwood 2014). To understand evolutionary diversification and model reef trophodynamics, more precise descriptions of parrotfish diets are required. Bonaldo et al. (2014) indicated that the nutritional targets for different species of parrotfishes require verification, and Wainwright and Price (2018) highlighted the paucity of detailed species-level information on feeding microhabitats and diet in parrotfishes. The present study is designed to address this knowledge gap.

The lack of clarity on parrotfish diets is partly due to the limitations of conventional gut content analysis for these fishes. Parrotfish lack a stomach, and ingested items in the anterior intestine are generally finely triturated by the pharyngeal apparatus (Ogden and Lobel 1978; Price et al. 2010), making identification difficult or impossible (Clements et al. 2017). Accordingly, our understanding of parrotfish diet is generally based on behavioural observations of the feeding substratum, rather than dietary/nutritional targets. This approach has led directly to parrotfishes being considered to eat macroalgae (e.g. Nakamura et al. 2003; Lefèvre and Bellwood 2011), live coral and sponges (e.g. Bonaldo et al. 2012; Burkepile et al. 2019), seagrass (e.g. Adam et al. 2015a, b) and algae on or within dead coral (e.g. Bruggemann et al. 1994a, b). Numerous studies conclude that parrotfish target macroalgae (Lewis 1985; Bonaldo et al. 2014; Mantyka and Bellwood 2007), although field studies indicate that patterns of parrotfish abundance and macroalgal cover are unrelated (Russ et al.

2015; Suchley et al. 2016; Bruno et al. 2019). Parrotfishes display very low levels of hindgut fermentation (Clements and Choat 1995; Crossman et al. 2005) and therefore lack the physiological capacity to digest phaeophytes efficiently (Clements et al. 2017; Clements and Choat 2018).

Recently, a synthetic hypothesis was proposed to explain parrotfish feeding behaviour, trophic anatomy, gut microbiota composition, levels of gastrointestinal fermentation, macronutrient composition of ingesta and stable isotope and fatty acid biomarkers, i.e. parrotfishes are microphages that target protein-rich epilithic, endolithic and epiphytic microscopic photoautotrophs, predominantly cyanobacteria (Clements et al. 2017; Clements and Choat 2018). This microphage hypothesis provides a unified explanation for the different feeding substrata targeted by parrotfishes, as calcareous substratum (both rock and sediment), macroalgae, seagrass, corals and sponges all provide habitats for microscopic photoautotrophs (Goldberg 2013). Clearly, testing this hypothesis requires resolving dietary targets at a microscopic level.

We examined the diversity, habit and abundance of epilithic, epiphytic and endolithic microphotoautotrophs on and in substrata targeted by parrotfishes. Since inventorying microscopic dietary items is not possible in situ (Adam et al. 2018), achieving our dietary resolution necessitated ‘bringing the reef to the microscope’. Previous studies used tiles or dead *Porites* to study successional communities (e.g. Scott and Russ 1987; Bruggemann et al. 1994a, b; McClanahan 1997; Tribollet et al. 2009); however, these are artificial substrata. Our solution was to extract cores around actual grazing targets of individual fish. Cores were analysed using microhistology (Garnick et al. 2018), enabling prey items to be identified and quantified. Prey assemblages could then be compared to previous studies cataloging temporal changes in epilithic and endolithic coral reef successional communities (e.g. Le Campion-Alsumard 1975; Le Campion-Alsumard et al. 1995; Chazottes et al. 1995; Diaz-Pulido and McCook 2002; Tribollet and Golubic 2005; Grange et al. 2015). Determining what was present at bite locations was designed to reveal interspecific variation in feeding selectivity in terms of both dietary biota and feeding substrata, shedding light on resource partitioning in parrotfish. We hypothesized that (a) microscopic photoautotrophs will be the most consistent and dominant elements of the core biota, and (b) parrotfish species will partition trophic resources by substratum taphonomy (Scoffin 1992).

Materials and methods

Core sampling protocol

Field sampling was conducted over 10 days in March 2018 within the Lizard Island Complex (14°40′ 4.13″ S, 145°27′ 45.14″ E), Great Barrier Reef, Australia. Sampling sites were selected based on known distribution and abundance of parrotfishes at Lizard Island (Supplementary Figure S1). Five species (*Scarus spinus*, *S. dimidiatus*, *S. frenatus*, *S. rivulatus* and *Chlorurus microrhinos*) were selected to represent both scraping (*Scarus* spp.) and excavating (*C. microrhinos*) taxa, with 19–21 replicate individuals sampled per species. Sampling was conducted during established peak feeding times for parrotfishes (Choat and Clements 1993). Terminal phase (TP) or large initial phase (IP) individuals were chosen haphazardly by the same experienced observer (KDC). Individual parrotfish were followed on snorkel until observed biting in rapid succession, known as a feeding foray (Bellwood and Choat 1990); then, an in situ photograph of the bite site (Supplementary Figure S2) was taken with a digital underwater camera (Nikon COOLPIX P900). The area surrounding the bite was then immediately extracted using a handheld brace with 22 mm diameter hole saw to an approximate depth of 2 cm. Each bite core was taken to the surface immediately and stored on ice in the boat. Upon return to the Lizard Island Research Station (1–3 h) cores were photographed then fixed in 70–80% ethanol. All further work took place at the University of Auckland.

Core indices

All 100 cores were parameterized along six indices: (1) substratum taphonomy (sensu Scoffin 1992), (2) maximum turf height, (3) epilith percentage surface cover, (4) species richness, (5) filamentous cyanobacteria density and (6) diatom density. A seventh index characterized the eendolith community (sensu Tribollet et al. 2009) for the excavator *C. microrhinos*.

Substratum taphonomy

Cores were assigned to one of five taphonomic categories: (1) recently dead coral without crustose coralline algae (CCA), (2) recently dead coral with CCA, (3) dead coral, partially white, (4) dead coral, white absent, surface hard, (5) dead coral, white absent, surface crumbly and highly bioeroded (Supplementary Figure S3).

Maximum turf height

The tallest biota on each core was photographed with an Infinity2 camera attached to a NIKON stereoscopic microscope, and its height was measured in mm (Maximum Turf Height) using Infinity Analyze software.

Epilithic biota percentage surface cover

Percentage surface cover of epilithic biota on each core was analysed using Coral Point Count (CPCe v4.1; Kohler and Gill 2006). A surface planar photograph was taken for each core at 5 × magnification (Supplementary Figure S4) and imported into CPCe. Planar surface area was measured using a Lumenera® Infinity 2 digital camera with Infinity Analyze.

Within CPCe a 7 × 7 grid was overlaid on the core surface and the biota under each point was identified. Taxa were coded to species where possible and totalled to provide a species richness score for each core. Live coral was not observed. Algae were assigned to the category turfing algae following Price and Scott (1992) and Connell et al. (2014). Cyanobacterial tufts were coded as separate to turfing algae and represented cyanobacterial filaments > 1 mm in length that were visible at 5 × magnification.

Cyanobacteria and diatom density

After the planar photograph, a 1 cm² × 1 mm deep scrape was taken from each core surface (Diaz-Pulido and McCook 2002; Bender et al. 2014). Each scrape sample was decalcified for 5 min with 10% HCl (Price and Scott 1992), centrifuged for 2 min at 2000 rpm. The resulting pellet was spread evenly onto a microscope slide, randomly distributed with a dissecting needle, then sealed under a 22 × 22 mm coverslip. A microscopic transect sampling procedure was devised to quantify all filamentous cyanobacteria and diatoms. Ten horizontal microscopic transects of the 22 mm × 22 mm coverslip were made at 630 × magnification. Diatoms were counted along each transect, and each cyanobacteria filament encountered was photographed using a Leica DC500 camera and measured lengthwise (Supplementary Figure S5) using Analysis LS Software. Cyanobacteria filament lengths were recorded for filamentous cyanobacteria.

Cyanobacteria cells were quantified by multiplying filament lengths by the *Species-specific cell: filament* ratio (Ssc:f). The Ssc:f value was derived as follows: the length of a cyanobacteria filament was measured and cells were counted for that length. The average of 10 filaments provided a different cell to filament ratio for each of the

cyanobacterial taxa encountered sensu Komárek et al. (2014).

Core euendolithic biota

Euendolithic biota from *C. microrhinos* cores was examined last. Excavating parrotfish possesses oral jaw myology and osteology which permits them to bite deeper into the substratum than scraping species (Bellwood and Choat 1990); therefore, endoliths accessible to *Chlorurus* were also examined. *Chlorurus microrhinos* cores were cut in half perpendicular to the core surface (Kiene and Hutchings 1994) using a Gryphon® diamond band saw. The halved cores were dried at 45 °C for 48 h before being vacuum embedded in a low viscosity epoxy resin (Golubic et al. 1970; Nielsen and Maiboe 2000). PetroThin sections were made then etched in 10% HCl and stained with 5% Toluidine blue (Tribollet and Payri 2001; Tribollet et al. 2009; Massé et al. 2018).

Sections were photographed at $100 \times -1000 \times$ using a Leica DC500 camera. Measurements were made in ImageJ. Euendoliths were identified by filament morphology following published literature (Humm and Wicks 1980; Le Campion-Alsumard et al. 1995; Tribollet et al. 2006, 2009; Gutner-Hoch and Fine 2011). To provide estimates of microborer depth, penetration and density, we measured: (1) the depth at which euendolith filaments were most abundant, i.e. Depth of Filament Abundance (D fa), and (2) the parameter P_{80} , a measure of the depth above which 80% of microboring filaments are observed (Tribollet et al. 2009).

Statistical analyses

Multivariate analysis of variance (MANOVA) was used to test the effect of species on the composition of epilithic core biota. Where significant differences were found, the MANOVA was then followed by separate one-way ANOVAs to describe variation among the five parrotfish species in each core variable. Post hoc Tukey's HSD all pairwise comparisons analyses were then used to locate the significant differences and identify homogeneous groupings within core biota categories. A principal component analysis was performed using the correlation coefficient matrix within the `prcomp` command in R statistical software (R Core Team 2018), as a means of dimension reduction for the nine parameters: CCA, cyanobacteria tufts, turf algae, *Dictyota* spp. and *Lobophora* spp., sponges, diatoms, epilithic biota species richness, maximum turf height and substratum taphonomy. To visualize trophic partitioning among the five scarine study species, centroid ellipses representing the species mean with 95%

confidence interval were superimposed on the PCA using the `vegan` package in R (Oksanen et al. 2018).

Results

A total of 100 cores were extracted at eight sites around the Lizard Island complex. The mean core surface area was $198 \pm 10.13 \text{ mm}^2$. Core surface area did not differ significantly among the five parrotfish species (one-way ANOVA, $p > 0.01$).

Variation in composition of epilithic biota

Thirty photoautotrophic taxa were identified across the 100 cores (Table 1). The two most frequently occurring epilithic photoautotrophs were filamentous cyanobacteria: *Calothrix confervicola* (Rivulariaceae) and *Lyngbya majuscula* (Oscillatoriales), present on 100% and 96% of cores, respectively. Surface cover of the nine epilithic parameters varied significantly among the five parrotfish species (Wilks' Lambda = 0.132, $F = 6.518$, $p < 0.0005$, Fig. 2, Supplementary Figure S7), although post hoc one-way ANOVA did not reveal interspecific differences in surface cover of *Dictyota*, *Jania adhaerens* or Ceramiales ($p > 0.05$).

Percentage cover of CCA varied significantly between parrotfish species (ANOVA, $F_{4,95} = 33.153$, $p = 0.0002$), with *S. spinus* cores having significantly more CCA on cores (Table 2) than any other parrotfish species ($p < 0.01$). Cyanobacteria tufts visible at 5x magnification had a mean surface area coverage of $27.9 \pm 2.5\%$, and coverage varied significantly among the five parrotfish species (ANOVA, $F_{4,95} = 27.461$, $p = 4.0756E - 7$), with *S. dimidiatus* cores having the greatest and *S. spinus* cores the least cyanobacteria tuft coverage (Tukey HSD post hoc, $p < 0.001$, Supplementary Figure S7).

The most abundant and frequently occurring (FO) algal species was the rhodophyte *Wurdemannia miniata* (Gigartinales, Solieriaceae), which was present on 65% of cores with a mean surface area coverage of $9.4 \pm 2.6\%$. The next most frequently occurring algal species was the rhodophyte *Herposiphonia secunda* f. *tenella* (Ceramiales, Rhodomelaceae) (53% of cores), covering an overall mean surface area of $4.7 \pm 1.5\%$.

Epilithic sponges were observed on 19/100 cores and were absent from *S. spinus* and *S. dimidiatus* cores. Sponge coverage differed significantly among the parrotfish species (ANOVA, $F_{4,95} = 6.537$, $p < 0.0001$), being greater on cores of *C. microrhinos* than *S. spinus*, *S. dimidiatus* or *S. frenatus* (Tukey HSD post hoc, $p < 0.01$).

Lobophora abscondita (Dictyotales, Zonarieae) was present on 26/100 cores, covering a total surface area of

Table 1 Heat map percentage frequency occurrence (%FO) of the BiteCore biota compared for the five scarini species

Surface Biota Observed on BiteCores					Percentage Frequency of Occurrence (%FO) of Biota on BiteCores											
Phylum	Class	Order	Family	Tribe	Genus species	<i>S. spinus</i>	<i>S. dimidiatus</i>	<i>S. frenatus</i>	<i>S. rivulatus</i>	<i>C. microrhinos</i>						
Cyanobacteria	Cyanophyceae	Nostocales	Rivulariaceae		<i>Calothrix confervicola</i>	100.0	100.0	100.0	100.0	100.00						
					>10,000 <i>C. confervicola</i> cells per 1cm ²	30.0	80.0	40.0	37.0	52.38						
		Hapalosiphonaceae			<i>Mastigocoleus testarum</i> Lagerheim	55.0	55.0	30.0	32.0	14.29						
					>1,000 <i>M. testarum</i> cells per 1cm ²	25.0	30.0	15.0	21.0	4.76						
		Oscillatoriales	Oscillatoriaceae			<i>Lyngbya majuscula</i>	85.0	100.0	100.0	95.0	100.00					
						>10,000 <i>L. majuscula</i> cells per 1cm ²	25.0	60.0	95.0	60.0	80.95					
		Spirulinales	Spirulinaceae			<i>Spirulina subsalsa</i>	10.0	35.0	4.0	37.0	33.33					
						> 1,000 <i>S. subsalsa</i> cells per 1cm ²	10.0	30.0	4.0	36.0	28.57					
		Rhodophyta	Florideophyceae	Corallinales	Corallinaceae		Crustose Coralline Algae	100.0	55.0	85.0	63.2	100.00				
							>50% coverage CCA	80.0	15.0	5.0	0.0	0.00				
Corallinales	Corallinaceae			Janieae		<i>Jania adhaerens</i>	5.0	10.0	60.0	63.2	71.43					
						Ceraminales	Ceramiaceae	Ceramiaceae		<i>Centroceras clavulatum</i>	0.0	0.0	10.0	15.8	9.52	
<i>Ceramium codii</i>	15.0			10.0	35.0					10.5	14.29					
<i>Ceramium flaccidum</i>	0.0			5.0	0.0					0.0	0.00					
<i>Ceramium isogonum</i>	0.0			0.0	5.0					10.5	4.76					
<i>Ceramium sympodiale</i>	5.0			5.0	5.0					5.3	9.52					
Rhodomelaceae	Herposiphoniaceae									<i>Herposiphonia secunda f. tenella</i>	33.3	35.0	85.0	73.7	52.38	
										Polysiphoniaceae	0.0	0.0	5.0	5.3	0.00	
Gigartinales	Delesseriaceae			Caloglosseae			<i>Taenioma nanum</i>	0.0	0.0	10.0	0.0	0.00				
							Wrangeliaceae	Griffithsiaceae			<i>Anotrichium tenue</i>	0.0	15.0	5.0	10.5	0.00
											Solieriaceae				<i>Wurdemannia miniata</i>	25.0
							Cystocloniaceae								<i>Hypnea spinella</i>	0.0
											Bacillariophyceae				Pennate Diatoms	100.0
		>100 diatoms per 1cm ²	35.0				95.0	100.0	95.0	18.00						
		Ochrophyta	Phaeophyceae				Dictyotales	Dictyotaceae	Dictyotaeae	<i>Dictyota dichotoma var. intricata</i>	0.0	0.0	5.0	0.0	4.76	
<i>Dictyota intermedia</i>	0.0			0.0	5.0	0.0				0.05						
Ectocarpales	Acinetosporaceae					<i>Lobophora abscondita</i>	10.0	0.0	55.0	37.0	28.57					
						<i>Feldmannia indica</i>	0.0	20.0	15.0	10.5	14.29					
Sphacelariales	Sphacelariaceae						<i>Feldmannia irregularis</i>	0.0	0.0	0.0	5.3	0.00				
							<i>Feldmannia mitchelliae</i>	5.0	0.0	30.0	0.0	0.00				
							<i>Sphacelaria Novae-Hollandiae</i>	0.0	5.0	15.0	0.0	0.00				
							<i>Sphacelaria rigidula</i>	0.0	0.0	5.0	0.0	0.00				
							<i>Sphacelaria rigidoides</i>	0.0	0.0	10.0	0.0	0.00				
							<i>Sphacelaria tribuloides</i>	0.0	0.0	10.0	0.0	0.00				
Chlorophyta	Ulvophyceae	Dasycladales	Polyphysaceae		<i>Parvocaulis parvulus</i>	0.0	0.0	5.0	0.0	0.00						
Porifera					Sponge Spicule Matrix	0.0	0.0	4.76	36.84	52.38						

Colour scale: single colour gradual percentage 0% White to 100% Red. This table combines all microscopy from 5× –1000× magnification for the 100 cores

6.2 ± 1.54% across the 100 cores. *L. abscondita* thalli were frequently epiphytized by the cyanobacterial taxa *Calothrix confervicola* and *Lyngbya majuscula*. Two filamentous phaeophytes were present (*Feldmannia* and *Sphacelaria*), covering 1.35 ± 0.3% of the total surface area across the 100 cores. *Dictyota dichotoma var. intricata* and *Dictyota intermedia* (Dictyotales, Dictyotaceae) were rare biota, only observed on four cores and combined had a mean overall surface area of (0.4 ± 0.2%). *Parvocaulis parvulus* (Dasycladales, Polyphysaceae) was the only epilithic chlorophyte observed and was only seen once on a *S. frenatus* core. The endolithic siphonous chlorophyte *Ostreobium* was observed in many *S. spinus* cores as a distinctive green band in the ‘fresh’ lab cross-sections under the live CCA crust and was recorded in the microscopic *C. microrhinos* endolith analysis to a depth of 3 mm in dead coral.

Species richness of core biota varied significantly between parrotfish species (ANOVA, $F_{4,95} = 19.58$, $p < 0.001$, Supplementary Figure S6). *Scarus spinus* and *S. dimidiatus* cores had significantly lower species richness

than cores of the other three parrotfish species (Tukey’s HSD, $p < 0.01$).

Substratum taphonomy

The taphonomy of the reefal substrata targeted by parrotfish varied significantly among the five study species. *Scarus dimidiatus* ($n = 20$) targeted significantly more ‘recently dead coral’ than the four other parrotfish species, while *C. microrhinos* ($n = 21$), *S. frenatus* ($n = 20$) and *S. rivulatus* ($n = 19$) targeted significantly more ‘highly bioeroded’ substratum than either *S. spinus* ($n = 20$) or *S. dimidiatus* (ANOVA, $F_{4,95} = 28.87$, $p < 0.001$; Fig. 1).

Maximum turf height

The mean maximum turf height across the 100 cores was 2.56 ± 0.23 mm. Maximum turf height differed significantly among the parrotfish species (ANOVA, $F_{4,95} = 2.693$, $p < 0.001$) (Fig. 2). Multiple pairwise comparisons revealed that *C. microrhinos* cores had

Table 2 Interspecific comparison of percentage surface cover for all epilithic BiteCore biota as determined by CPCE (means ± SE)

BiteCore Biota Percent Surface Cover				<i>S. spinus</i>	<i>S. dimidiatus</i>	<i>S. frenatus</i>	<i>S. rivulatus</i>	<i>C. microrhinos</i>		
Phylum	Class	Order	Family	Species	Mean % (SE)	Mean % (SE)	Mean % (SE)	Mean % (SE)	Mean % (SE)	
Cyanobacteria				Cyanobacteria tufts (spp.)	6.68 (± 3.91)	56.73 (± 4.83)	24.32 (± 3.18)	29.41 (± 5.57)	22.86 (± 3.41)	
Rhodophyta		Corallinales	Corallinales	Crustose coralline algae (spp.)	76.77 (± 6.18)	18.93 (± 6.00)	19.67 (± 4.84)	8.64 (± 2.38)	26.88 (± 3.00)	
Florideophyceae	Gigartinales	Solieriaceae		<i>Jania adhaerens</i>	0.36 (± 0.36)	0.74 (± 0.56)	4.42 (± 1.20)	7.17 (± 3.35)	6.74 (± 1.69)	
				<i>Wurdemannia miniata</i>	1.10 (± 0.47)	7.61 (± 2.10)	17.04 (± 1.20)	13.07 (± 3.28)	9.51 (± 2.22)	
	Cerariales	Rhodomelaceae		<i>Hypnea spinella</i>	–	–	0.19 (± 0.19)	6.12 (± 3.97)	5.24 (± 1.66)	
				<i>Herposiphonia secunda f. tenella</i>	2.10 (± 0.89)	1.91 (± 0.66)	7.08 (± 1.47)	8.57 (± 2.48)	4.38 (± 1.40)	
	Ceramiaceae			<i>Polysiphonia isogona</i>	4.10 (± 1.35)	5.96 (± 1.72)	0.75 (± 0.37)	–	2.17 (± 1.27)	
				<i>Polysiphonia scopulorum</i>	3.91 (± 3.69)	2.34 (± 1.35)	1.92 (± 1.20)	2.68 (± 0.83)	1.95 (± 0.77)	
				<i>Polysiphonia amphibolis</i>	–	–	0.16 (± 0.16)	0.28 (± 0.28)	–	
				<i>Ceramium codii</i>	1.02 (± 0.58)	0.31 (± 0.22)	1.44 (± 0.45)	0.62 (± 0.43)	0.60 (± 0.33)	
				<i>Ceramium sympodiale</i>	0.65 (± 0.48)	0.19 (± 0.19)	0.16 (± 0.16)	0.15 (± 0.15)	0.39 (± 0.27)	
				<i>Ceramium isogonum</i>	–	–	0.16 (± 0.16)	0.55 (± 0.38)	0.18 (± 0.18)	
				<i>Ceramium virgatum</i>	–	0.21 (± 0.21)	–	–	–	
				<i>Centroceras clavulatum</i>	–	–	0.65 (± 0.46)	1.03 (± 0.59)	1.12 (± 0.93)	
	Wrangeliaceae			<i>Anotrichium tenue</i>	–	0.55 (± 0.30)	0.10 (± 0.10)	0.85 (± 0.61)	–	
				<i>Taenioma nanum</i>	–	–	0.48 (± 0.40)	–	–	
	Ochrophyta, Phaeophyceae	Ectocarpales	Acinetosporaceae		<i>Feldmannia mitchelliae</i>	0.22 (± 0.22)	–	1.18 (± 0.49)	–	–
					<i>Feldmannia indica</i>	–	1.66 (± 0.84)	0.60 (± 0.33)	0.67 (± 0.46)	0.60 (± 0.33)
Sphacelariales		Sphacelariaceae		<i>Feldmannia irregularis</i>	–	–	–	0.29 (± 0.29)	–	
				<i>Sphacelaria novae-hollandiae</i>	–	0.22 (± 0.22)	0.63 (± 0.35)	–	–	
				<i>Sphacelaria rigidula</i>	–	–	0.28 (± 0.28)	–	–	
				<i>Sphacelaria tribuloides</i>	–	–	0.41 (± 0.29)	–	–	
Dictyotales		Dictyotaceae		<i>Lobophora abscondita</i>	2.69 (± 2.50)	–	13.97 (± 5.07)	9.07 (± 4.31)	5.64 (± 2.46)	
				<i>Dictyota dichotoma var. intricata</i>	–	–	1.15 (± 1.15)	–	0.21 (± 0.21)	
				<i>Dictyota intermedia</i>	–	–	0.22 (± 0.22)	–	0.25 (± 0.25)	
				<i>Parvocaulis parvulus</i>	–	–	0.19 (± 0.19)	–	–	
Chlorophyta	Ulvophyceae	Dasycladales		–	–	0.25 (± 0.30)	3.07 (± 1.37)	6.60 (± 2.09)		
Porifera			Sponge	–	1.84 (± 1.84)	–	5.73 (± 4.04)	1.51 (± 1.03)		
Other categories				Dead Coral	–	–	–	–	1.61 (± 0.80)	
				Macroborer Hole	0.41 (± 0.30)	0.81 (± 0.48)	0.41 (± 0.30)	1.36 (± 0.683)	0.21 (± 0.21)	
				Snail, Sipunculids	–	–	0.53 (± 0.40)	0.29 (± 0.22)	0.21 (± 0.21)	
				Polychaetes	–	–	1.17 (± 0.60)	0.39 (± 0.27)	1.02 (± 0.61)	
				Unknowns	–	–	0.47 (± 0.20)	–	0.32 (± 0.22)	

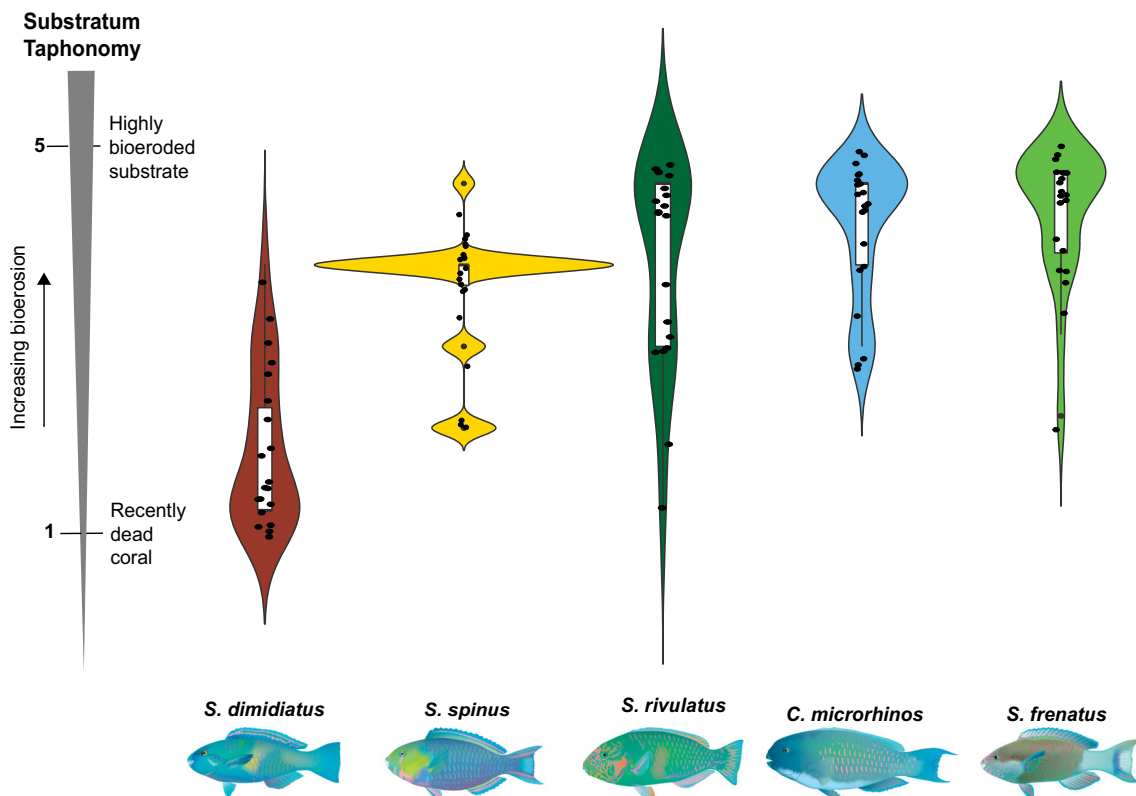


Fig. 1 Violin plot showing substratum taphonomy. Datapoints represent each individual core and boxplot to visualize core variation between parrotfish species. Box lines are the 75th and 25th percentiles, and whiskers are values within 1.5 times interquartile range

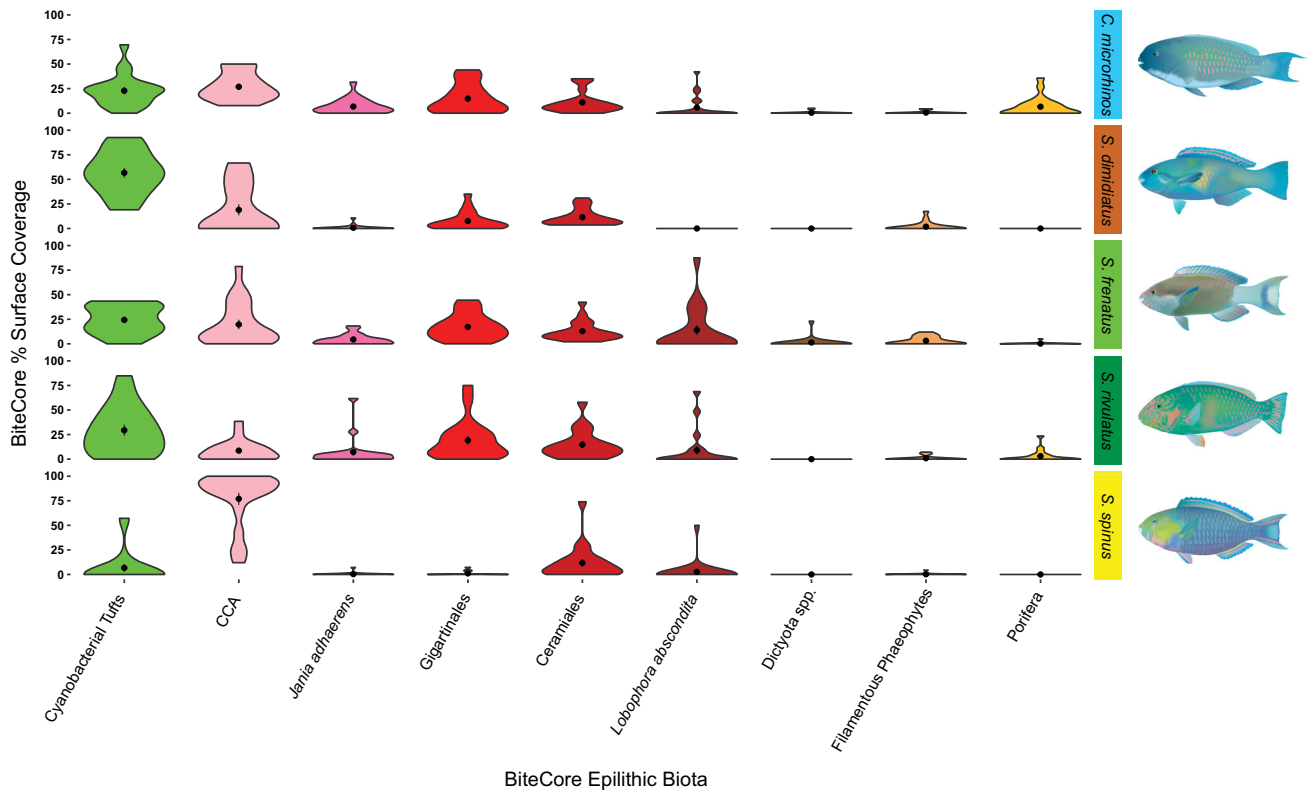


Fig. 2 Violin plot showing core biota percentage surface cover visible at 5 × magnification. Species means are indicated with a black dot for nine epilithic taxa for each of the five parrotfishes. Column colour indicates biota

significantly taller turf than cores of both *S. dimidiatus* and *S. spinus* (Table 3).

Filamentous cyanobacteria counts

The total number of filamentous cyanobacteria cells on the cores measured at 630x did not vary between parrotfish species (ANOVA, $F_{4,95} = 1.674, p = 0.162$, Fig. 3). *Lynghya majuscula* was observed on 96% of the cores (Table 1) and was the most abundant filamentous cyanobacterium overall (mean $31,034 \pm 4647$ cells/cm²). The heterocystous *Calothrix confervicola* was the second

most abundant filamentous cyanobacterium overall (mean $18,680 \pm 2542$ cells/cm²) and was present on all 100 cores. *Spirulina subsalsa* had a mean abundance of 2215 ± 825 cells/cm², present on 27% of the cores. *Mastigocoleus testarum* was the least abundant filamentous cyanobacterium (1147 ± 431 cells/cm²) observed on 37/100 cores.

Pennate diatom counts

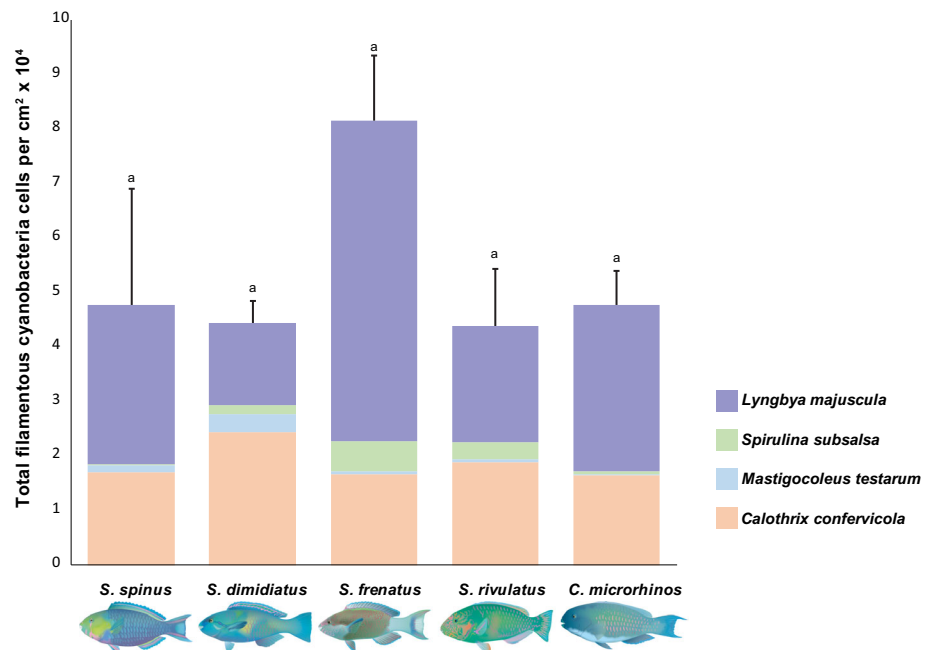
Pennate diatoms (Ochrophyta, Bacillariophyceae) were present on 100% of cores (Table 1) with an overall average

Table 3 Maximum turf height for the BiteCores compared for the five scarini species

Max turf height	Mean ± SE (mm)	Min–Max (mm)	Tukey post hoc ($p < 0.001$)	Species and order of tallest biota
<i>C. microrhinos</i> (n = 21)	4.10 ± 0.54	1.2–12.9	c	<i>Hypnea spinella</i> (Gigartinales)
<i>S. rivulatus</i> (n = 19)	3.43 ± 0.54	1.2–10.6	bc	<i>Hypnea spinella</i> (Gigartinales)
<i>S. frenatus</i> (n = 20)	3.03 ± 0.36	0.5–7.0	abc	<i>Wurdemannia miniata</i> (Gigartinales)
<i>S. dimidiatus</i> (n = 20)	1.44 ± 0.23	0.4–4.3	ab	<i>Wurdemannia miniata</i> (Gigartinales)
<i>S. spinus</i> (n = 20)	0.78 ± 0.12	0.0–1.9	a	<i>Polysiphonia isogona</i> (Cerariales)

Means ± SE and sample range (mm). The tallest biota from each core (n = 100) was measured and identified to species. Tukey’s HSD Post-Hoc homogenous subsets are indicated ($p < 0.001$)

Fig. 3 Mean (+SE) cyanobacteria cell counts per 1 cm² core for the five parrotfish species at 630 × magnification. Lower case letters indicate homogeneous subsets (Tukey's HSD post hoc multiple comparison of means test, $p < 0.05$). Colours indicate cyanobacteria taxa



of 544 ± 95 cells per 1 cm². *Scarus rivulatus* cores had significantly more diatoms than those of *S. dimidiatus* and *S. spinus* (ANOVA, $F_{4,95} = 4.242$, $p = 0.0033$).

Endolithic microbial community in *Chlorurus microrhinos* cores

Fifteen *C. microrhinos* cores were suitable for sectioning to examine the microendolithic community. The six remaining cores were too fragmentary to section. The microchlorophyte *Ostreobium* spp. dominated the endolithic assemblages of *C. microrhinos* cores (Table 4) and was observed to penetrate to 3 mm. The euendolithic cyanobacteria *Hyella caespitosa* (Pleurocapsales) and *Mastigocoleus testarum* (Nostocales) were observed very rarely.

Principal component analysis

Principal component analysis (PCA) was conducted on the nine epilithic parameters (Fig. 4; Table 5). PC1 (30.5%) was negatively associated with maximum turf height, turf algae coverage and species richness, and clustered *S. spinus* and *S. dimidiatus* together, and separated them from

the other three parrotfish species. PC2 (20.9%) was positively associated with CCA and taphonomy and negatively associated with cyanobacterial tufts and partitioned *S. dimidiatus* from *S. spinus*. PC3 (13.4% variance) was positively correlated with cyanobacteria tufts, *Dictyota* and *Lobophora*, and negatively associated with sponge density (Fig. 4). *Scarus frenatus*, *S. rivulatus* and *C. microrhinos* cluster together on the basis of their significantly taller turf, more highly bioeroded substratum and greater species richness.

Discussion

Our novel bite core microhistology method enabled both microscopic and macroscopic prey taxa of parrotfishes to be identified and quantified. The dominant functional groups of epilithic biota on the cores were tufted cyanobacteria, turfing algae and crustose coralline algae (CCA). The only consistent feature across all cores was the high density of filamentous cyanobacteria, supporting the view that these parrotfishes target microphotoautotrophs. Macroalgae was absent or a minor component on cores, supporting the hypothesis that these parrotfishes avoid

Table 4 Euendolith penetration depth parameters for *Chlorurus microrhinos* BiteCores (n = 15) 4 depth measurements per core at 100 × magnification

Endolith depth	Maximal density mean ± SE (mm)	P ₈₀ density mean ± SE (mm)
<i>Chlorurus microrhinos</i> BiteCores	1.02 ± 0.003	1.08 ± 0.020

larger algae. We discuss each of these dietary components in more detail below.

Filamentous cyanobacteria

The core microscopy supported the hypothesis that microscopic photoautotrophs are a consistent and dominant component of parrotfish feeding targets. Cyanobacteria were present as (a) epilithic tufts visible at $5 \times$ magnification, (b) microscopic filaments occurring as biofilm on CCA, unattached in turf and attached as epiphytes on turfing algae and macroalgae, and (c) euendolithic filaments. Furthermore, our data revealed that study parrotfish species partitioned this prolific microscopic trophic resource primarily by the taphonomy of feeding substrata. Macroscopic rhodophytes and phaeophytes, including components of algal turf, were inconsistent components of the epilithic core biota, with the exception of CCA in *S. spinus* and *C. microrhinos*. CCA comprised much greater surface coverage than tufted cyanobacteria on cores of *S. spinus*, which nonetheless contained similar high densities of microscopic filamentous epilithic and endolithic cyanobacteria to the other species' cores due to the cyanobacterial biofilm on CCA.

We note that the surface cover on our cores of cyanobacterial tufts is much greater, and macroalgae even lower, than historically reported for general benthic community composition in comparable reef habitats at Lizard Island (Hoey and Bellwood 2010). Bleaching episodes at Lizard Island result in increases in cyanobacterial cover (Wismer et al. 2019). However, the mean coverage of cyanobacterial tufts reported for peak bleaching in quadrats where tufts were present was 23.9% (Wismer et al. 2019), below the mean coverage recorded across the 100 cores in the present study ($27.9 \pm 2.5\%$). These previous studies were conducted using field-based surveys and did not resolve the composition of the benthic biota at a microscopic scale. 'Bringing the reef to the microscope' allowed us to identify the relevant biota and also examine the relationship between the biotic composition and the taphonomy of the substratum. All of these elements are necessary to understand parrotfish diets.

Based on our microhistology, *Lyngbya* and *Calothrix* were the dominant filamentous cyanobacteria on cores, with *Mastigocoleus testarum* and *Spirulina* present but at low abundance. This is consistent with previous studies at Lizard Island (Burris 1976; Borowitzka et al. 1978; Larkum et al. 1988; Tribollet 2008), indicating that these cyanobacteria are well-established members of the reef biota. *Lyngbya* and *Calothrix* are dominant biota in early successional epilithic communities (Tsuda and Kami 1973), supporting the view that some parrotfishes target early successional photoautotrophs (Clements et al. 2017).

Lyngbya majuscula has been identified in blooms in Queensland, Florida and the Caribbean (Albert et al. 2005; Paul et al. 2005; O'Neil et al. 2012), and sequences related to *Lyngbya* were recovered from all cyanobacterial mats sampled in Curaçao (Brocke et al. 2018). *Lyngbya majuscula* has been identified as toxic to humans (Osborne et al. 2001; Taylor et al. 2014) and was thought to deter feeding in some herbivorous fishes including parrotfish (Nagle and Paul 1999; Capper et al. 2016). Secondary metabolite content can vary within cyanobacterial taxa, and the extent of deterrence can vary with previous exposure (Thacker et al. 1997; Thacker and Paul 2004). The abundance of *Lyngbya* on bite cores raises the question of whether (a) the strains consumed have any post-ingestive effect on parrotfish, or (b) parrotfish can detoxify the secondary metabolites involved. Ongoing molecular work will examine whether 'toxic' strains are present on parrotfish bite cores.

The presence of *Calothrix confervicola* on all cores is consistent with work by Diaz-Pulido and McCook (2002) who found *Calothrix* present on all their bleached coral samples. Our microscopy revealed the morphological plasticity and habits of *C. confervicola*. It presented as an epiphytic biofilm on CCA, an epilithic biofilm on recently dead coral, an epiphyte on *Wurdemannia miniata* and a false-branched tuft.

Other epilithic biota

The macroalgae *Turbinaria*, *Sargassum*, *Halimeda*, *Galaxaura*, *Padina* and *Amphiroa* were not observed on any cores, but are all present at the study location (Hoey and Bellwood 2010). *Dictyota* was observed on only four cores, i.e. *S. frenatus* and *C. microrhinos*. The mean maximum turf height for the 100 cores was 2.6 mm, consistent with the sparse turf category sensu Bruggemann et al. (1994b). This adds weight to the hypothesis that these parrotfish target and maintain turfs in early successional states. The repeated grazing of sites, as evident in our in situ photographs (Supplementary Fig. 2), confirms that sites are re-grazed, creating a renewable source of protein-rich primary production in the form of fast growing filamentous microphotoautotrophs.

Trophic resource partitioning

An unexpected finding was that *S. spinus* cores were predominantly covered in CCA (i.e. 75% of *S. spinus* cores had over 85% CCA coverage), indicating that *S. spinus* targets CCA (Fig. 5). CCA itself is of low nutritional value (Montgomery and Gerking 1980; Bruggemann et al. 1994a). However, our microscopy revealed that CCA on the cores hosted abundant filamentous cyanobacteria as

both biofilm and euendoliths, with the result that *S. spinus* did not differ from the other species in total cyanobacterial cell counts. Both *Lyngbya majuscula* and *C. confervicola* were observed as an epiphytic biofilm on CCA, consistent with 16S rRNA barcoding studies which identified cyanobacteria in CCA biofilm (Webster et al. 2013; Sneed et al. 2015). Our microscopy also revealed that the euendolithic cyanobacterium *Mastigocoleus testarum* was present within CCA, consistent with earlier studies (Tribollet and Payri 2001; Chazottes et al. 2002). *Scarus spinus* cores varied in successional taphonomy, consistent with the fact that CCA colonizes bare substratum 20 days after coral mortality and can be dominant in later successional states (Littler and Littler 2013). Our finding that *S. spinus* targeted CCA biofilm challenges the prevailing view that parrotfishes are generalist algal turf feeders and indicates that this parrotfish feeds highly selectively.

Our taphonomic analysis also provided evidence that trophic resource partitioning involved successional stage of the substratum, e.g. 95% of *S. dimidiatus* cores were recently dead coral. This substratum preference was unique to *S. dimidiatus* and implies that this parrotfish is also highly selective. These very early successional cores displayed low species richness, consistent with early successional communities (Odum 1969). *Scarus dimidiatus* cores had high surface coverage of cyanobacteria tufts, consistent with studies of successional communities where filamentous cyanobacteria are pioneering biota (e.g. Grange et al. 2015). Recently dead cores were the only successional stage where *C. confervicola* was the dominant filamentous cyanobacterium. The euendolithic cyanobacterium *M. testarum* was also at its highest abundance on *S. dimidiatus* cores, consistent with previous observations of *M. testarum* within days of coral death (Le Campion-Alsumard et al. 1995; Grange et al. 2015). The filamentous rhodophytes *Polysiphonia* and *Herposiphonia* were also observed colonizing these primary successional substrata, being characterized by creeping lateral axes and attachment rhizoids. Filamentous rhodophytes are of high nutritional value, being rich in protein and essential fatty acids (Clements and Choat 2018). This is potentially important as some essential long-chain fatty acids are absent in cyanobacteria (Lang et al. 2011).

Scarus frenatus and *S. rivulatus* cores were similar in taphonomy and biota except for the greater density of *L. majuscula* in the former. This overlap of parameters indicates that these two species target similar substrata. These two species exhibit distinct habitat partitioning in continental shelf position and habitat selection on mid-shelf reefs (Russ 1984) and displayed low functional overlap in microhabitat use at Lizard Island (Brandl and Bellwood 2014). Foraging behaviour also differs, with *S. frenatus* usually foraging in pairs on the reef crest or outer flat of

Fig. 4 Principal component biplot of PC1 and PC2 (a) and PC2 and PC 3 (b) with loadings arrows for the nine core indices. Shaded areas represent the 95% confidence interval around species means for the five parrotfish species. Dots represent individual cores ($n = 100$). Colours represent the five parrotfish species

mid- and outer-shelf reefs, while *S. rivulatus* graze in multi-specific groups in a wider range of habitats including sedimented reef flats on the inner shelf (Cheal et al. 2012). Trophic resource partitioning among study parrotfishes therefore seems to be driven by multiple factors including habitat, foraging microhabitat and substratum taphonomy, while dietary targets per se are relatively consistent (i.e. microscopic photoautotrophs). The substrata targeted by the excavator *C. microrhinos* were consistently highly bioeroded, displaying higher species richness, tallest maximum turf height and greatest sponge coverage. These characteristics indicate that *C. microrhinos* cores are at a later successional stage than substrata targeted by the other parrotfishes.

Endolithic community

The results from the petrograph-thin endolith microscopy revealed that the microboring photoautotrophic (endolith) communities in the *C. microrhinos* cores were dominated by the siphonous chlorophyte *Ostreobium*. *Ostreobium* spp. become the dominant endoliths in experimental CaCO_3 blocks at the final dissolution stage, defined as a ‘mature’ endolithic community, after five to twelve months of exposure (Gektidis 1999; Tribollet et al. 2009; Grange et al. 2015). The microchlorophyte *Phaeophila dendroides* was not observed. *Phaeophila dendroides* and the boring cyanobacteria *Mastigocoleus testarum* dominate the euendolith community in the first 3 months of succession (Le Campion-Alsumard et al. 1995; Grange et al. 2015). The penetration depth of *Ostreobium* observed in the *C. microrhinos* cores and its dominance in the endolithic assemblage indicate that the substrates targeted by this excavating parrotfish were late succession communities (Chazottes et al. 1995; Grange et al. 2015). The depth of the excavating bite of *C. microrhinos* would allow access to the full penetration depth of *Ostreobium* in these late succession endolith communities.

Heavily bioeroded reef yields a greater density of euendoliths, which are major sources of primary productivity within dead carbonate substrata (Tribollet et al. 2006). This represents a valuable trophic resource only accessible to parrotfish possessing the oral jaw morphology necessary to excavate carbonate substrata (Bellwood and Choat 1990; Wainwright and Price 2018). The morphological specializations of excavators are consistent with endolithic rather than epilithic dietary targets (cf. Nanami

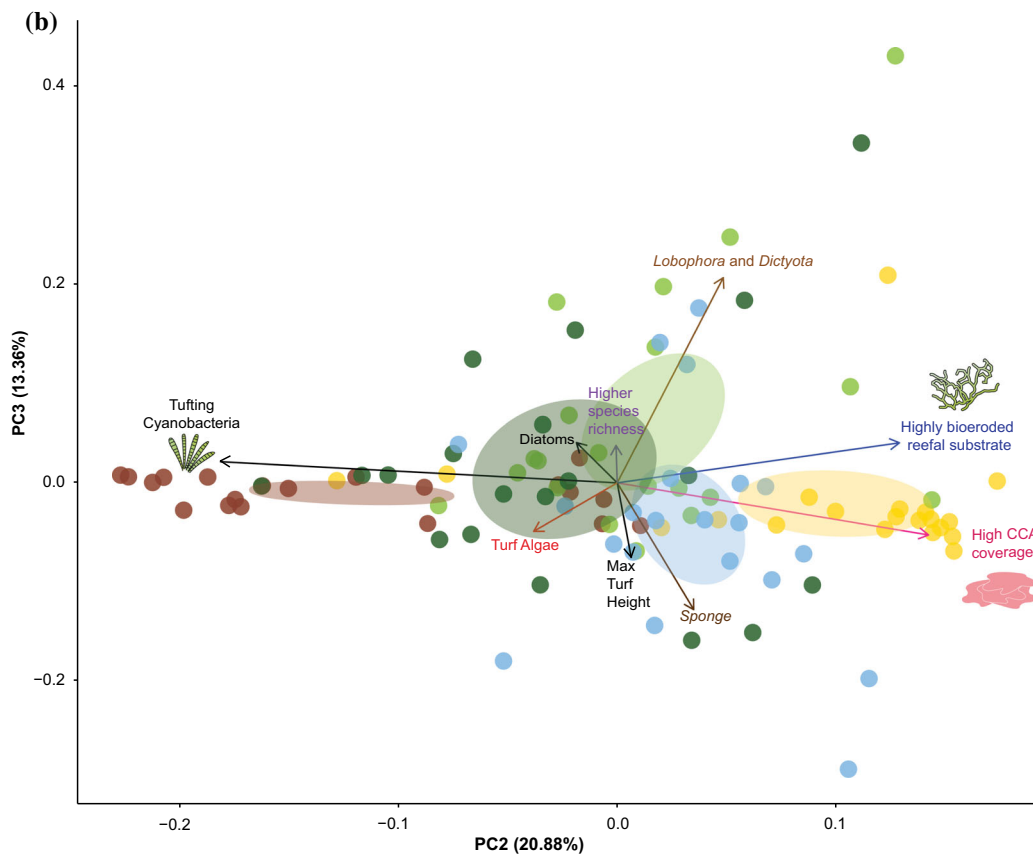
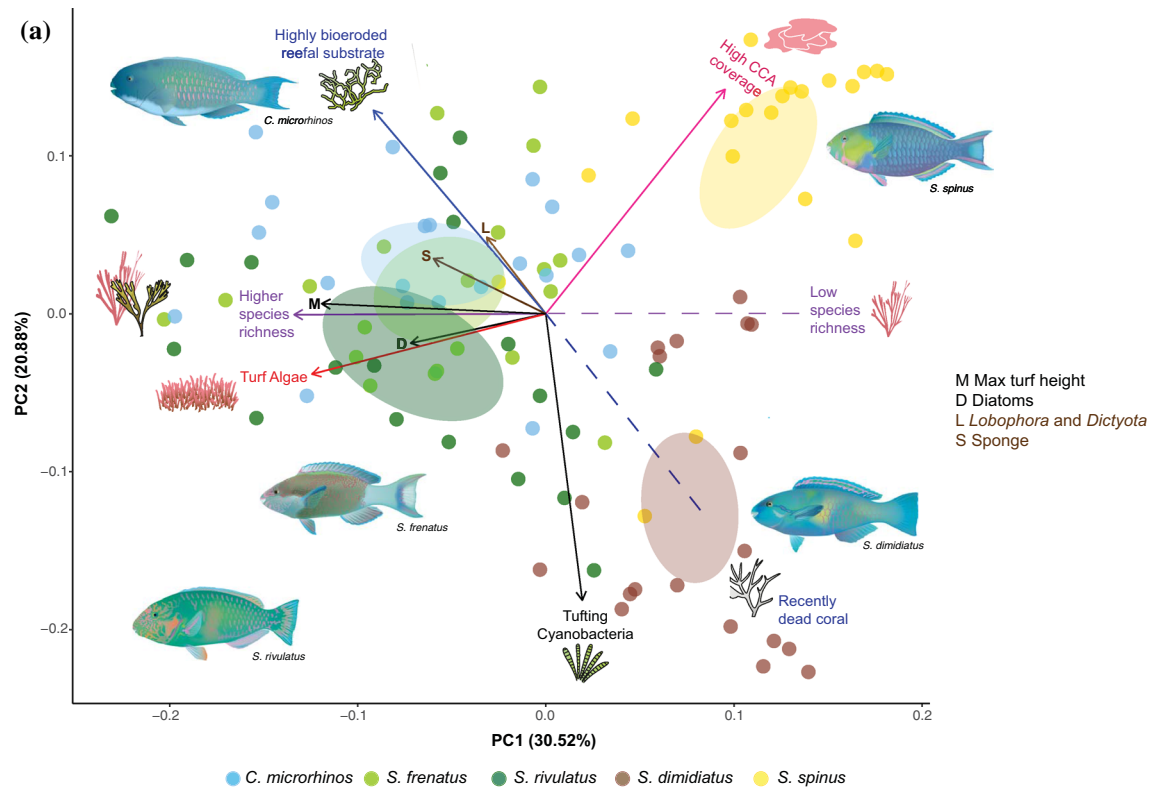


Table 5 Principal component analysis on nine BiteCore parameters loadings over 0.4 in bold. Percent of total variance for each principal component shown

	PC1 30.5%	PC2 20.9%	PC3 13.4%
Cyanobacteria tuft	0.07077	– 0.66179	0.77896
CCA	0.34770	0.51859	– 0.19184
Dictyota and Lobophora	– 0.11448	0.17669	0.75401
Porifera	– 0.21785	0.12757	– 0.46654
Reefal substrate	– 0.33439	0.47016	0.14740
Diatoms	– 0.26196	– 0.06790	0.14819
Species richness	– 0.48832	– 0.00202	0.13753
Max turf height	– 0.43456	0.02344	– 0.27655
Turf algae	– 0.45364	– 0.13923	– 0.17849

2016; Carlson et al. 2017). The high relative abundance of *Ostreobium* observed in this study explains the difference in depleted $\delta^{15}\text{N}$ previously reported between scrapers and excavators (Plass-Johnson et al. 2013), as *Ostreobium* is not diazotrophic (i.e. does not fix nitrogen) and so does not generate the depleted ^{15}N signal characteristic of cyanobacteria (Clements and Choat 2018).

Methodology for diet studies

By incorporating both microscopic and macroscopic food resources, our core method adds a critical layer of detail missing from previous studies on parrotfish dietary targets. Both feeding observations based on visual benthic surveys and most gut content analyses to date fail to capture the microscopic taxa that appear to be critical elements of parrotfish diets. Stable isotope and fatty acid biomarker approaches are both informative in terms of qualitative assessments of diet (Clements et al. 2017), but not quantitative diet composition. Another method that has been



Fig. 5 *Scarus spinus* (terminal phase) scraping CCA biofilm at Toberua Island, Fiji. Photograph KDC

suggested to add taxonomic breadth to coral reef trophodynamic studies is diet metabarcoding (Casey et al. 2019; Stamoulis et al. 2017). However, the inability to quantify dietary items in terms of biomass or relative abundance (Nielsen et al. 2017) makes diet metabarcoding problematic for characterizing complex, phylogenetically disparate diets such as those of parrotfishes. Biases among potential prey taxa in gene copy number, DNA extraction and amplification (Alberdi et al. 2019; Deagle et al. 2019; Lamb et al. 2019) and contamination of ingesta with environmental DNA (Shinzato et al. 2018; Alexander et al. 2020) currently limit metabarcoding approaches.

Conclusion

Our qualitative and quantitative microhistology analysis of parrotfish bite cores is a novel approach to characterizing the nutritional targets of grazing reef fishes. Our data provide additional support for the hypothesis that parrotfish target high-protein microscopic photoautotrophs, particularly cyanobacteria. Our finding of highly selective trophic resource partitioning of these microscopic primary producers among these sympatric parrotfishes challenges: (a) the notion of parrotfishes as generalist herbivores on EAM and (b) the utility for trophodynamic studies on grazing reef fishes of observational feeding studies that rely on heterogeneous resource categories such as EAM or turfing algae. Our data indicate that trophic specialization in these fishes involves selection at small spatial scales of feeding substrata (especially stage of taphonomic succession) rather than diet specialization per se. Future work involves expanding the approach described here to increase the number of parrotfish species examined and broaden the level of spatial and temporal sampling.

Acknowledgements We thank Anne Hoggett and Lyle Vail for their help at the Lizard Island Research Station. We also thank Adrian Turner for assistance with microscopy, Wendy Nelson for algal identification, Aline Tribollet for assistance with the endolith analysis, Paul Kench for help with coring technique and coral reef taphonomy, Andrés Arcila-Rivera for the use of petrography equipment, Vivian Ward for graphic design and Howard Choat for helpful comments. Comments from the editor and two anonymous reviewers improved this paper.

Compliance with ethical standards

Conflict of interest On behalf of all authors, the corresponding author states that there is no conflict of interest.

References

- Adam T, Burkepile D, Ruttenberg B, Paddock JM (2015a) Herbivory and the resilience of Caribbean coral reefs: knowledge gaps and implications for management. *Mar Ecol Prog Ser* 520:1–20
- Adam TC, Kelley M, Ruttenberg BI, Burkepile DE (2015b) Resource partitioning along multiple niche axes drives functional diversity in parrotfishes on Caribbean coral reefs. *Oecologia* 179:1173–1185
- Adam T, Duran A, Fuchs C, Roycroft M, Rojas M, Ruttenberg B, Burkepile D (2018) Comparative analysis of foraging behavior and bite mechanics reveals complex functional diversity among Caribbean parrotfishes. *Mar Ecol Prog Ser* 597:207–220
- Alberdi A, Aizpuru O, Bohmann K, Gopalakrishnan S, Lynggaard C, Nielsen M, Gilbert MTP (2019) Promises and pitfalls of using high-throughput sequencing for diet analysis. *Mol Ecol Resour* 19:327–348
- Albert S, O’Neil JM, Udy JW, Ahern KS, O’Sullivan CM, Dennison WC (2005) Blooms of the cyanobacterium *Lyngbya majuscula* in coastal Queensland, Australia: disparate sites, common factors. *Mar Pollut Bull* 51:428–437
- Alexander JB, Bunce M, White N, Wilkinson SP, Adam AAS, Berry T, Stat M, Thomas L, Newman SJ, Dugal L, Richards ZT (2020) Development of a multi-assay approach for monitoring coral diversity using eDNA metabarcoding. *Coral Reefs* 39:159–171
- Bellwood DR, Choat JH (1990) A functional analysis of grazing in parrotfishes (family Scaridae): the ecological implications. *Environ Biol Fishes* 28:189–214
- Bellwood DR, Hoey AS, Ackerman JL, Depczynski M (2006) Coral bleaching, reef fish community phase shifts and the resilience of coral reefs. *Glob Chang Biol* 12:1587–1594
- Bellwood DR, Hughes TP, Folke C, Nyström M (2004) Confronting the coral reef crisis. *Nature* 429:827–833
- Bellwood DR, Tebbett SB, Bellwood O, Mihalitsis M, Morais RA, Streit RP, Fulton CJ (2018) The role of the reef flat in coral reef trophodynamics: past, present, and future. *Ecol Evol* 8:4108–4119
- Bender D, Diaz-Pulido G, Dove S (2014) Warming and acidification promote cyanobacterial dominance in turf algal assemblages. *Mar Ecol Prog Ser* 517:271–284
- Bonaldo RM, Hoey AS, Bellwood DR (2014) The ecosystem roles of parrotfishes on tropical reefs. *Oceanogr Mar Biol Annu Rev* 52:81–132
- Bonaldo RM, Welsh JQ, Bellwood DR (2012) Spatial and temporal variation in coral predation by parrotfishes on the GBR: evidence from an inshore reef. *Coral Reefs* 31:263–272
- Borowitzka MA, Larkum AWD, Borowitzka LJ (1978) A preliminary study of algal turf communities of a shallow coral reef lagoon using an artificial substratum. *Aquat Bot* 5:365–381
- Bozec Y-M, O’Farrell S, Bruggemann JH, Luckhurst BE, Mumby PJ (2016) Tradeoffs between fisheries harvest and the resilience of coral reefs. *Proc Natl Acad Sci* 113:4536–4541
- Brandl SJ, Bellwood DR (2014) Individual-based analyses reveal limited functional overlap in a coral reef fish community. *J Anim Ecol* 83:661–670
- Brocke HJ, Piltz B, Herz N, Abed RMM, Palinska KA, John U, Den Haan J, De Beer D (2018) Nitrogen fixation and diversity of benthic cyanobacterial mats on coral reefs in Curaçao. *Coral Reefs* 37:861–874
- Bruggemann JH, Kuyper MWM, Breeman AM (1994a) Comparative analysis of foraging and habitat use by the sympatric Caribbean parrotfish *Scarus vetula* and *Sparisoma viride* (Scaridae). *Mar Ecol Prog Ser* 112:51–66
- Bruggemann JH, van Oppen MJH, Breeman AM (1994b) Foraging by the stoplight parrotfish *Sparisoma viride*. I. Food selection in different, socially determined habitats. *Mar Ecol Prog Ser* 106:41–55
- Bruno JF, Côté IM, Toth LT (2019) Climate change, coral loss, and the curious case of the parrotfish paradigm: Why don’t marine protected areas improve reef resilience? *Ann Rev Mar Sci* 11:307–334
- Burkepile DE, Adam TC, Roycroft M, Ladd MC, Munsterman KS, Ruttenberg BI (2019) Species-specific patterns in corallivory and spongivory among Caribbean parrotfishes. *Coral Reefs* 38:417–423
- Burris R (1976) Nitrogen fixation by blue-green algae of the Lizard Island area of the Great Barrier Reef. *Aust J Plant Physiol* 3:41–51
- Capper A, Erickson AA, Ritson-Williams R, Becerro MA, Arthur KA, Paul VJ (2016) Palatability and chemical defences of benthic cyanobacteria to a suite of herbivores. *J Exp Mar Biol Ecol* 474:100–108
- Carlson PM, Davis K, Warner RR, Caselle JE (2017) Fine-scale spatial patterns of parrotfish herbivory are shaped by resource availability. *Mar Ecol Prog Ser* 577:165–176
- Casey JM, Meyer CP, Morat F, Brandl SJ, Planes S, Parravicini V (2019) Reconstructing hyperdiverse food webs: gut content metabarcoding as a tool to disentangle trophic interactions on coral reefs. *Methods Ecol Evol* 10:1157–1170
- Chazottes V, Le Campion-Alsumard T, Peyrot-Clausade M (1995) Bioerosion rates on coral reefs: interactions between macroborers, microborers and grazers (Moorea, French Polynesia). “Palaeogeography. Palaeoclimatol Palaeoecol 113:189–198
- Chazottes V, Le Campion Alsumard T, Peyrot-Clausade M, Cuet P (2002) The effects of eutrophication-related alterations to coral reef communities on agents and rates of bioerosion (Reunion Island, Indian Ocean). *Coral Reefs* 21:375–390
- Cheal A, Emslie M, Miller I, Sweatman H (2012) The distribution of herbivorous fishes on the Great Barrier Reef. *Mar Biol* 159:1143–1154
- Choat JH (1991) The biology of herbivorous fishes on coral reefs. In: Sale PF (ed) *The ecology of fishes on coral reefs*. Academic Press, San Diego, pp 120–155
- Choat JH, Clements KD (1993) Daily feeding rates in herbivorous labroid fishes. *Mar Biol* 117:205–211
- Chung AE, Wedding LM, Green AL, Friedlander AM, Goldberg G, Meadows A, Hixon MA (2019) Building coral reef resilience through spatial herbivore management. *Front Mar Sci* 6:1–12
- Clements KD, Choat JH (1995) Fermentation in tropical marine herbivorous fishes. *Physiol Zool* 68:355–378
- Clements KD, Choat JH (2018) Nutritional ecology of parrotfishes (Scarinae, Labridae). In: Hoey AS, Bonaldo RM (eds) *Biology of parrotfishes*. CRC Press, Boca Raton, pp 42–68
- Clements KD, German DP, Piché J, Tribollet A, Choat JH (2017) Integrating ecological roles and trophic diversification on coral reefs: multiple lines of evidence identify parrotfishes as microphages. *Biol J Linn Soc* 120:729–751
- Connell SD, Foster MS, Airoidi L (2014) What are algal turfs? Towards a better description of turfs. *Mar Ecol Prog Ser* 495:299–307
- Crossman DJ, Choat JH, Clements KD (2005) Nutritional ecology of nominally herbivorous fishes on coral reefs. *Mar Ecol Prog Ser* 296:129–142
- Deagle BE, Thomas AC, McInnes JC, Clarke LJ, Vesterinen EJ, Clare EL, Kartzinel TR, Eveson JP (2019) Counting with DNA in metabarcoding studies: How should we convert sequence reads to dietary data? *Mol Ecol* 28:391–406
- Diaz-Pulido G, McCook LJ (2002) The fate of bleached corals: patterns and dynamics of algal recruitment. *Mar Ecol Prog Ser* 232:115–128

- Garnick S, Barboza PS, Walker JW (2018) Assessment of animal-based methods used for estimating and monitoring rangeland herbivore diet composition. *Rangel Ecol Manag* 71:449–457
- Gektidis M (1999) Cyanobacteria and associated microorganisms characterize coarse shoreline carbonates of One Tree Island, Australia. *Bull l'Institut Oceanogr* 19:127–133
- Goldberg WM (2013) *The biology of reefs and reef organisms*. University of Chicago Press, Chicago
- Golubic S, Brent G, Lecampion T (1970) Scanning electron microscopy of endolithic algae and fungi using a multipurpose casting-embedding technique. *Lethaia* 3:203–209
- Grange JS, Rybarczyk H, Tribollet A (2015) The three steps of the carbonate biogenic dissolution process by microborers in coral reefs (New Caledonia). *Environ Sci Pollut Res* 22:13625–13637
- Gutner-Hoch E, Fine M (2011) Genotypic diversity and distribution of *Ostreobium quekettii* within scleractinian corals. *Coral Reefs* 30:643–650
- Hoey AS, Bellwood DR (2010) Among-habitat variation in herbivory on *Sargassum* spp. on a mid-shelf reef in the northern Great Barrier Reef. *Mar Biol* 157:189–200
- Hughes TP, Rodrigues MJ, Bellwood DR, Ceccarelli D, Hoegh-Guldberg O, McCook L, Moltschaniwskij N, Pratchett MS, Steneck RS, Willis B (2007) Phase shifts, herbivory, and the resilience of coral reefs to climate change. *Curr Biol* 17:360–365
- Humm HJ, Wicks SR (1980) *Introduction and guide to the marine bluegreen algae*. John Wiley and Sons, New York
- Jones CG, Gutiérrez JL, Byers JE, Crooks JA, Lambrinos JG, Talley TS (2010) A framework for understanding physical ecosystem engineering by organisms. *Oikos* 119:1862–1869
- Jones CG, Lawton JH, Shachak M (1994) Organisms as ecosystem engineers. *Oikos* 69:373
- Kiene WE, Hutchings PA (1994) Bioerosion experiments at Lizard Island, Great Barrier Reef. *Coral Reefs* 13:91–98
- Kohler KE, Gill SM (2006) Coral point count with excel extensions (CPCe): a visual basic program for the determination of coral and substrate coverage using random point count methodology. *Comput Geosci* 32:1259–1269
- Komárek J, Kaštovský J, Mareš J, Johansen JR (2014) Taxonomic classification of cyanoprokaryotes (cyanobacterial genera) 2014, using a polyphasic approach. *Preslia* 86:295–335
- Lamb PD, Hunter E, Pinnegar JK, Creer S, Davies RG, Taylor MI (2019) How quantitative is metabarcoding: a meta-analytical approach. *Mol Ecol* 28:420–430
- Lang I, Hodac L, Friedl T, Feussner I (2011) Fatty acid profiles and their distribution patterns in microalgae: a comprehensive analysis of more than 2000 strains from the SAG culture collection. *BMC Plant Biol* 11:124
- Larkum AWD, Kennedy IR, Muller WJ (1988) Nitrogen fixation on a coral reef. *Mar Biol* 98:143–155
- Le Campion-Alsumard T (1975) Experimental study of the colonization of calcite fragments by marine endolithic Cyanophyceae. *Cah Biol Mar* 16:177–185
- Le Campion-Alsumard T, Golubić S, Hutchings P (1995) Microbial endoliths in skeletons of live and dead corals: *porites lobata* (Moorea, French Polynesia). *Mar Ecol Prog Ser* 117:149–157
- Lefèvre CD, Bellwood DR (2011) Temporal variation in coral reef ecosystem processes: herbivory of macroalgae by fishes. *Mar Ecol Prog Ser* 422:239–251
- Lewis SM (1985) Herbivory on coral reefs: algal susceptibility to herbivorous fishes. *Oecologia* (Berlin) 65:370–375
- Littler MM, Littler SD (2013) The nature of crustose coralline algae and their interactions on reefs. *Smithson Contrib Mar Sci* 39:199–212
- Mallela J, Fox RJ (2018) The role of parrotfishes in the destruction and construction of coral reefs. In: Hoey AS, Bonaldo RM (eds) *Biology of parrotfishes*. CRC Press, Boca Raton, pp 161–196
- Mantyka CS, Bellwood DR (2007) Direct evaluation of macroalgal removal by herbivorous coral reef fishes. *Coral Reefs* 26:435–442
- Massé A, Domart-Coulon I, Golubic S, Duché D, Tribollet A (2018) Early skeletal colonization of the coral holobiont by the microboring Ulvophyceae *Ostreobium* sp. *Sci Rep* 8:2293
- McClanahan TR (1997) Primary succession of coral-reef algae: differing patterns on fished versus unfished reefs. *J Exp Mar Bio Ecol* 218:77–102
- Melgarejo-Damián MP, González-Acosta AF, Cruz-Escalona VH, Moncayo-Estrada R (2018) A comparison of feeding biomechanics between two parrotfish species from the Gulf of California. *Zoomorphology* 137:165–176
- Montgomery WL, Gerking SD (1980) Marine macroalgae as foods for fishes: an evaluation of potential food quality. *Environ Biol Fishes* 5:143–153
- Morgan KM, Kench PS (2016) Parrotfish erosion underpins reef growth, sand talus development and island building in the Maldives. *Sediment Geol* 341:50–57
- Mumby PJ (2006) The impact of exploiting grazers (Scaridae) on the dynamics of Caribbean coral reefs. *Ecol Appl* 16:747–769
- Mumby PJ, Dahlgren CP, Harborne AR, Kappel CV, Micheli F, Brumbaugh DR, Holmes KE, Mendes JM, Broad K, Sanshirico JN, Buch K, Box S, Stoffle RW, Gill AB (2006) Fishing, trophic cascades, and the process of grazing on coral reefs. *Science* 311:98–101
- Nagle DG, Paul VJ (1999) Production of secondary metabolites by filamentous tropical marine cyanobacteria: ecological functions of the compounds. *J Phycol* 35:1412–1421
- Nakamura Y, Horinouchi M, Nakai T, Sano M (2003) Food habits of fishes in a seagrass bed on a fringing coral reef at Iriomote Island, southern Japan. *Ichthyol Res* 50:15–22
- Nanami A (2016) Parrotfish grazing ability: interspecific differences in relation to jaw-lever mechanics and relative weight of adductor mandibulae on an Okinawan coral reef. *PeerJ* 4:e2425
- Nielsen JK, Maiboe J (2000) Epofix and vacuum: an easy method to make casts of hard substrates. *Palaeontol Electron* 3:10
- Nielsen JM, Clare EL, Hayden B, Brett MT, Kratina P (2017) Diet tracing in ecology: method comparison and selection. *Methods Ecol Evol* 9:278–291
- O'Neil JM, Davis TW, Burford MA, Gobler CJ (2012) The rise of harmful cyanobacteria blooms: the potential roles of eutrophication and climate change. *Harmful Algae* 14:313–334
- Odum EP (1969) The strategy of ecosystem development. *Science* 164:262–270
- Odum HT, Odum EP (1955) Trophic structure and productivity of a windward coral reef community on Eniwetok Atoll. *Ecol Monogr* 25:291–320
- Ogden JC, Lobel PS (1978) The role of herbivorous fishes and urchins in coral reef communities. *Environ Biol Fishes* 3:49–63
- Oksanen J, Blanchet FG, Kindt R, Legendre P, Minchin PR, O'hara RB, Simpson GL, Solymos P, Stevens MHH, Wagner H (2018) Package 'vegan' community ecology package. See www.cranr-project.org/web/packages/vegan/index.html
- Ong L, Holland KN (2010) Bioerosion of coral reefs by two Hawaiian parrotfishes: species, size differences and fishery implications. *Mar Biol* 157:1313–1323
- Osborne NJT, Webb PM, Shaw GR (2001) The toxins of *Lyngbya majuscula* and their human and ecological health effects. *Environ Int* 27:381–392
- Paul VJ, Thacker RW, Banks K, Golubic S (2005) Benthic cyanobacterial bloom impacts the reefs of South Florida (Broward County, USA). *Coral Reefs* 24:693–697
- Perry CT, Kench PS, O'Leary MJ, Morgan KM, Januchowski-Hartley F (2015) Linking reef ecology to island building: parrotfish

- identified as major producers of island-building sediment in the Maldives. *Geology* 43:503–506
- Plass-Johnson JG, McQuaid CD, Hill JM (2013) Stable isotope analysis indicates a lack of inter- and intra-specific dietary redundancy among ecologically important coral reef fishes. *Coral Reefs* 32:429–440
- Price I, Scott F (1992) The turf algal flora of the Great Barrier Reef Part I. Rhodophyta. James Cook University of North Queensland, Townsville
- Price SA, Wainwright PC, Bellwood DR, Kazancioglu E, Collar DC, Near TJ (2010) Functional innovations and morphological diversification in parrotfish. *Evolution (N Y)* 64:3057–3068
- Russ G (1984) Distribution and abundance of herbivorous grazing fishes in the central Great Barrier Reef. II. Patterns of zonation of mid-shelf and outershelf reefs. *Mar Ecol Prog Ser* 20:35–44
- Russ GR, Questel S-LA, Rizzari JR, Alcalá AC (2015) The parrotfish–coral relationship: refuting the ubiquity of a prevailing paradigm. *Mar Biol* 162:2029–2045
- Scoffin TP (1992) Taphonomy of coral reefs: a review. *Coral Reefs* 11:57–77
- Scott FJ, Russ GR (1987) Effects of grazing on species composition of the epilithic algal community on coral reefs of the central Great Barrier Reef. *Mar Ecol Prog Ser* 39:293–304
- Shinzato C, Zayasu Y, Kanda M, Kawamitsu M, Satoh N, Yamashita H, Suzuki G (2018) Using seawater to document coral-zoothanellae diversity: a new approach to coral reef monitoring using environmental DNA. *Frontiers Mar Sci* 5:28
- Sneed JM, Ritson-Williams R, Paul VJ (2015) Crustose coralline algal species host distinct bacterial assemblages on their surfaces. *ISME J* 9:2527–2536
- Stamoulis KA, Friedlander AM, Meyer CG, Fernandez-Silva I, Toonen RJ (2017) Coral reef grazer-benthos dynamics complicated by invasive algae in a small marine reserve. *Sci Rep* 7:43819
- Steneck RS (1983) Escalating herbivory and resulting adaptive trends in calcareous algal crusts. *Paleobiology* 9:44–61
- Steneck RS, Arnold SN, Mumby PJ (2014) Experiment mimics fishing on parrotfish: insights on coral reef recovery and alternative attractors. *Mar Ecol Prog Ser* 506:115–127
- Steneck RS, Bellwood DR, Hay ME (2017) Herbivory in the marine realm. *Curr Biol* 27:R484–R489
- Steneck RSS (1995) Is herbivore loss more damaging to reefs than hurricanes? Case studies from two Caribbean reef systems (1978–1988). *Oceanogr Lit Rev* 9:778–779
- Stuart-Smith RD, Bates AE, Lefcheck JS, Duffy JE, Baker SC, Thomson RJ, Stuart-Smith JF, Hill NA, Kininmonth SJ, Airoidi L, Becerro MA, Campbell SJ, Dawson TP, Navarrete SA, Soler GA, Strain EMA, Willis TJ, Edgar GJ (2013) Integrating abundance and functional traits reveals new global hotspots of fish diversity. *Nature* 501:539–542
- Suchley A, McField MD, Alvarez-Filip L (2016) Rapidly increasing macroalgal cover not related to herbivorous fishes on Mesoamerican reefs. *PeerJ* 4:e2084
- Taylor MS, Stahl-Timmins W, Redshaw CH, Osborne NJ (2014) Toxic alkaloids in *Lyngbya majuscula* and related tropical marine cyanobacteria. *Harmful Algae* 31:1–8
- Thacker RW, Paul VJ (2004) Morphological, chemical, and genetic diversity of tropical marine cyanobacteria *Lyngbya* spp. and *Symploca* spp. (Oscillatoriales). *Appl Environ Microbiol* 70:3305–3312
- Thacker RW, Nagle DG, Paul VJ (1997) Effects of repeated exposures to marine cyanobacterial secondary metabolites on feeding by juvenile rabbitfish and parrotfish. *Mar Ecol Prog Ser* 147:21–29
- Tribollet A (2008) Dissolution of dead corals by euendolithic microorganisms across the Northern Great Barrier Reef (Australia). *Microb Ecol* 55:569–580
- Tribollet A, Godinot C, Atkinson M, Langdon C (2009) Effects of elevated pCO₂ on dissolution of coral carbonates by microbial euendoliths. *Global Biogeochem Cycles* 23:1–7
- Tribollet A, Golubic S (2005) Cross-shelf differences in the pattern and pace of bioerosion of experimental carbonate substrates exposed for 3 years on the northern Great Barrier Reef, Australia. *Coral Reefs* 24:422–434
- Tribollet A, Langdon C, Golubic S, Atkinson M (2006) Endolithic microflora are major primary producers in dead carbonate substrates of Hawaiian coral reefs. *J Phycol* 42:292–303
- Tribollet A, Payri C (2001) Bioerosion of the coralline alga *Hydrolithon onkodes* by microborers in the coral reefs of Moorea, French Polynesia. *Oceanol Acta* 24:329–342
- Tsuda RT, Kami HT (1973) Algal succession on artificial reefs in a marine lagoon environment in Guam. *J Phycol* 9:260–264
- Wainwright PC, Price SA (2018) Innovation and diversity of the feeding mechanism in parrotfishes. In: Hoey AS, Bonaldo RM (eds) *Biology of parrotfishes*. CRC Press, Boca Raton, pp 26–41
- Webster NS, Uthicke S, Botté ES, Flores F, Negri AP (2013) Ocean acidification reduces induction of coral settlement by crustose coralline algae. *Glob Chang Biol* 19:303–315
- Williams GJ, Graham NAJ, Jouffray J-B, Norström AV, Nyström M, Gove JM, Heenan A, Wedding LM (2019) Coral reef ecology in the Anthropocene. *Funct Ecol* 33:1014–1022
- Wilson SK, Bellwood DR, Choat JH, Furnas MJ (2003) Detritus in the epilithic algal matrix and its use by coral reef fishes. *Oceanogr Mar Biol* 41(41):279–309
- Wismer S, Tebbett SB, Streit RP, Bellwood DR (2019) Spatial mismatch in fish and coral loss following 2016 mass coral bleaching. *Sci Total Environ* 650:1487–1498

Publisher's Note Springer Nature remains neutral with regard to jurisdictional claims in published maps and institutional affiliations.